A Mathematical Model for Longitudinal Bone Growth



Richard Hall

Corpus Christi College

University of Oxford

A dissertation submitted in partial fulfilment
of the requirements for the degree of

Master of Science

September 2000

To my family.

Acknowledgements

First and foremost I would like to thank my two supervisors, Andrew Fowler and Philip Maini, for presenting me with this fascinating problem, for many fruitful discussions and meetings, and for their diligence in ploughing through the many drafts of this dissertation. Thanks as well to Cornelia Farnum, for starting the ball rolling, and for providing most of the relevant data. I am most indebted to Jill Urban for her constructive criticism of the model, and for providing an invaluable introduction to bone biology. Finally, I would like to express my gratitude to the Engineering and Physical Sciences Research Council for their financial support over the last twelve months.

Contents

1 Introduction **1**

1.1 Elementary growth plate dynamics 2

1.2 Factors affecting bone growth 4

1.3 Motivation for a mathematical model 5

2 Setting up the Model **8**

2.1 Overview 8

2.2 Derivation of the governing equations 9

2.3 Boundary conditions at $z = h(t)$. 13

2.4 Boundary conditions at $z = b(t)$. 14

2.5 Nondimensionalisation 14

2.6 Sizes of the dimensionless parameters. 17

3 Model Analysis **19**

3.1 The leading-order model 19

3.2 Steady state solution 20

3.3 Comparison with data 26

4 Discussion and Conclusion **29**

4.1 Review of dissertation 29

4.2 Model limitations and directions for future research 30

Bibliography **32**

Chapter 1

Introduction

From birth through to adolescence, long bones (such as the tibia and radius) grow by the process of endochondral ossification (derived from the Greek *endon* + *chondros* 'within cartilage' and the Latin *os* + *facere* 'to make bone'). The process is so-called because a bone increases in length only via the growth plate cartilage located at its ends [17]. One of the most interesting aspects of endochondral ossification is the phenomenon of differential bone growth. Different amounts and rates of growth are observed in different bones in the same animal, and even at opposite ends of the same bone. In 28-day-old rats, for example, the average daily growth rate of the proximal tibia is up to eight times greater than that of the proximal radius [18].

The cells in the growth plate also demonstrate a strong horizontal zonation, i.e. if a cross-section of the growth plate is taken perpendicular to the long axis of the bone, the cells populating it will all have similar properties. In the following section we outline the highly structured transitions that the cells comprising the growth plate undergo to produce bone. Inevitably there will be a significant amount of medical jargon: rather than cluttering the text with definitions, I have included a glossary of medical terms as an appendix.

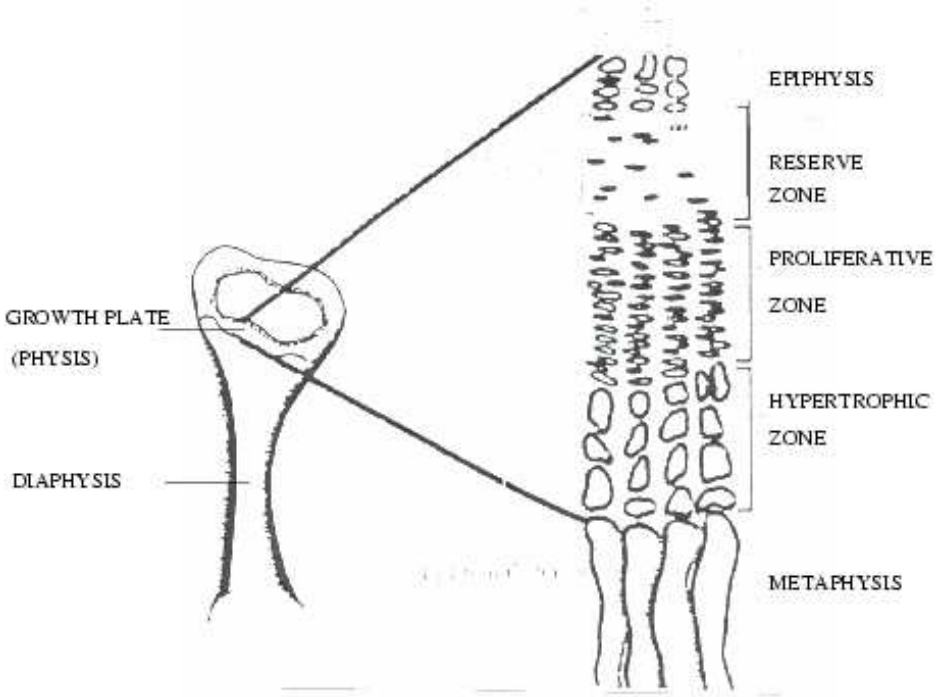


Figure 1.1: The basic structure of a long bone and growth plate.

1.1 Elementary growth plate dynamics

For our purposes, the long bone can be thought of as consisting of a main shaft (the diaphysis) with a growth plate (physis) at each end (Fig. 1.1). The physis is sandwiched between two regions of bone: the bone contiguous to the main shaft is called the metaphysis, and that furthest from the shaft (on the other side of the physis) is called the epiphysis. The epiphyseal bone, which forms separately from the diaphysis, is known as a secondary centre of ossification. For convenience we adopt the following terminology: the direction parallel to the long axis of the bone will be referred to as the vertical, and that perpendicular to the axis the horizontal. The base of the growth plate is taken to be the (chondro-osseous) junction of the physis and metaphysis.

Growth plate cartilage consists of three phases: the cartilage cells (chondrocytes), solid matrix, and interstitial fluid. Solid matrix is synthesized by the chondrocytes, and is made up of fibrillar and nonfibrillar collagens, small and large proteoglycans, and various non-collagenous proteins [10]. The interstitial fluid, which occupies approximately seventy per cent of the extracellular volume of the growth plate, is pri-

marily water containing small solutes such as glucose. The physis is avascular, and all nutrients are provided by the blood supply to the epiphysis. Nutrients then progress through the growth plate via diffusion.

Growth plate activity begins in the cartilage near the epiphysis. The chondrocytes in this region are randomly oriented and are not dividing. Some of the cells here will act as germinal or stem cells to the growth plate, others will ultimately form the articular cartilage present in all adult joints. This region is known as the *reserve cell zone*.

At the base of the reserve cell zone, stem cells are stimulated to induce mitosis (asexual cell replication). The ensuing region in which cell division occurs is called the *proliferative zone*. A characteristic of this region is that the cells are aligned in vertical columns. The cells are typically squat (wider than they are long relative to the columnar orientation). All cells in this zone are capable of division, and do so at least once [5]. Cell proliferation maintains steady growth of the bone (the number of cells produced here offsets the number lost at the metaphysis). The solid matrix is also organized into two distinct components [9]: the pericellular (territorial) matrix surrounding individual cells, and interterritorial matrix which occurs between cell columns. The collagen fibrils in the interterritorial matrix are vertically oriented, and help to maintain the columnar structure of the cells (Fig. 1.2).

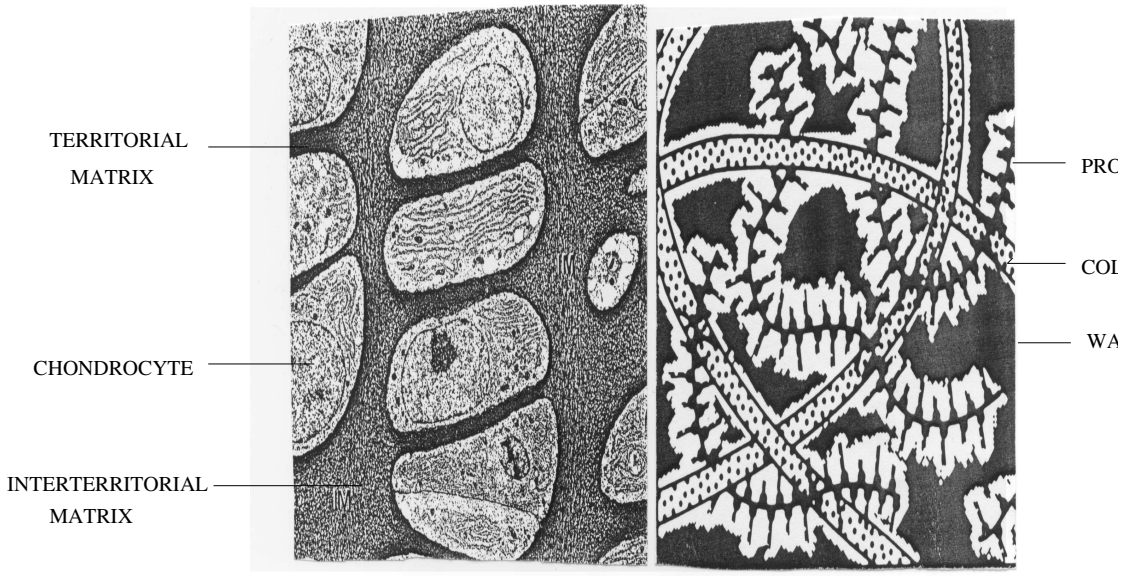


Figure 1.2: A close-up of the cells and matrix in the growth plate (left), and microscopic view of the solid matrix in the interstitial fluid. Pictures from [9], [13].

During the next transitional phase, the cells stop dividing and begin to increase in volume with a preferential increase in cell height (*i.e.* in the direction of bone growth) - this phenomenon is known as hypertrophy and the corresponding region is called the *hypertrophic cell zone*. This region accounts for most of the overall growth observed in the bone, with some cells swelling to approximately ten times their original volume [2].

Towards the base of the hypertrophic zone, the interterritorial matrix undergoes calcification. At the chondro-osseous junction between the growth plate and the metaphyseal bone, the remaining unmineralized cartilage is destroyed, along with roughly two-thirds of the mineralized matrix. The remaining matrix acts as a scaffold for bone deposition. The fate of the chondrocytes at the chondro-osseous junction is unclear, though current opinion [10] is that they die by apoptosis (programmed cell death). Capillaries can now invade the volume formerly occupied by the chondrocytes, bringing osteoblasts (bone-producing cells) to the base of the growth plate.

Once the desired bone length has been attained, cell proliferation tails off while the cell removal rate at the metaphysis remains constant. This causes the physis to shrink and eventually disappear, so the physis is essentially a transient organ.

1.2 Factors affecting bone growth

Longitudinal bone growth is controlled by a number of factors, which can be placed into two broad categories: biological and mechanical. Biological inputs include nutrients (*e.g.* glucose, oxygen) carried to the growth plate via the bloodstream. A variety of signalling molecules are involved in the activation of the different behaviours of the chondrocytes. Some of these are produced by the endocrine system and arrive via the circulation: these include growth hormone (which stimulates growth factors), thyroid hormone (promotes chondrocyte maturation and hypertrophy) and vitamin D [15]. Autocrine/paracrine molecules (produced locally at the growth plate) include insulin-like growth factors (to augment matrix synthesis), fibroblast and transforming growth factors (stimulate chondrocyte proliferation) and bone morphogenetic proteins (induce bone formation).

Mechanical effects also play an important part in determining the extent and rate of bone growth. Current experimental techniques for altering bone growth [4] include compression via the insertion of a staple (Fig. 1.3A) around the growth plate. Rapid declines are observed in the number of chondrocytes contributing to growth, and in the height of hypertrophic cells. Conversely, distraction across a growth plate results in bone lengthening. It is achieved by epiphyseolysis (whereby a large distractive force over a short time is used to fracture the growth plate) or by chondrodiastasis (a smaller force applied over a longer period of time avoiding growth plate fracture). These procedures are thought to affect bone growth by promoting or inhibiting blood flow to the epiphysis, and hence nutrient supply to the growth plate [1].

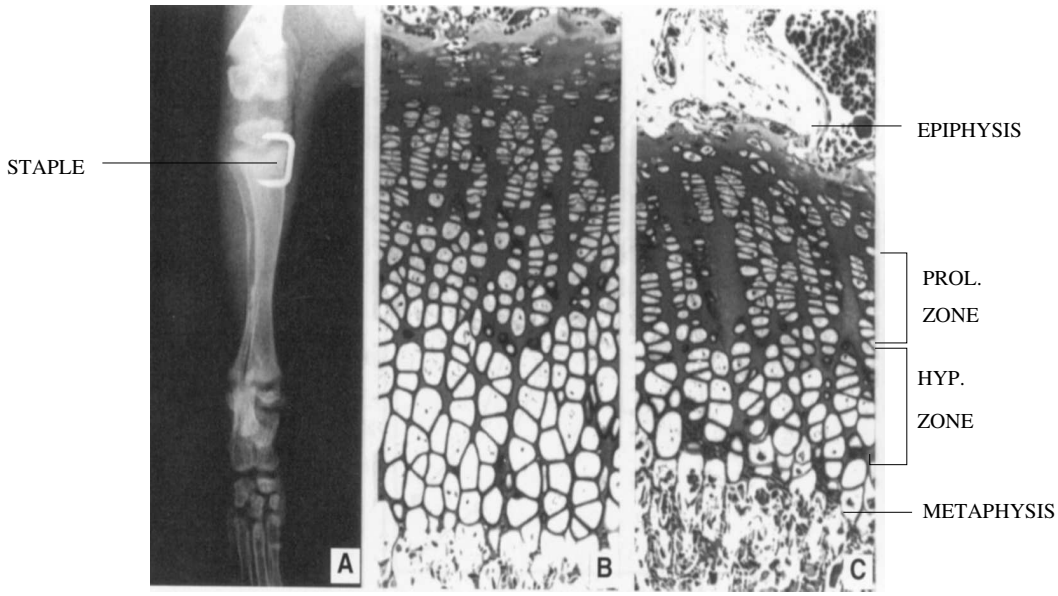


Figure 1.3: The effect of stapling on the proximal tibia of a four-week-old rat. The physis of the unstapled limb (B) and the stapled limb (C) six days after implantation. Pictures from [4].

1.3 Motivation for a mathematical model

Skeletal growth in mammals is a tightly-controlled process which operates on two levels: local formation of a highly-structured growth plate and global coordination of all the growth plates in the body. However, there is scope for a number of things to go wrong, resulting in deformities in one, and occasionally several, of the bones

(Fig. 1.4). Commonly occurring abnormalities include gigantism or overgrowth of a limb or digit, hypoplasia (undergrowth) and dysplasia (abnormal growth resulting in misshapen joints) [8].

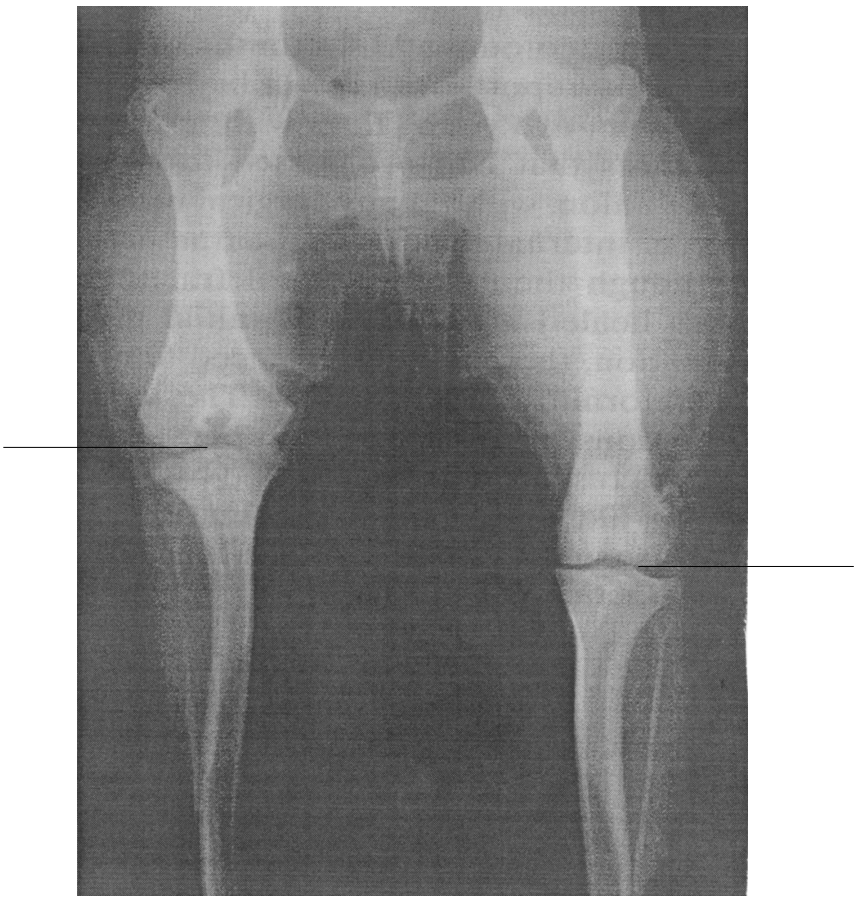


Figure 1.4: X-ray of a dog with a growth abnormality. The total leg length is the same for each leg, but the knee joints are at different heights (highlighted by the horizontal lines). Undergrowth of the femur has been compensated for by the overgrowth of the tibia. Picture provided by C.E. Farnum.

A mathematical model of endochondral ossification would help us to identify which of the regulatory parameters are most important in determining the amount and rate of growth at a physis, and would hopefully explain how differential longitudinal growth is possible at opposite ends of the same bone. A deeper understanding of the cellular dynamics of bone growth could also suggest strategies for treatment of growth plate abnormalities.

In Chapter 2, we present a simple one-dimensional, triphasic model for growth plate

dynamics, whereby the onset of proliferative and hypertrophic behaviour of cells is controlled by the level of a generic growth factor diffusing through the physis. In Chapter 3 we look for steady-state solutions to the leading-order problem, and compare our results with the available data. A discussion of the model and its limitations, as well as directions for further research, is included in Chapter 4.

Chapter 2

Setting up the Model

2.1 Overview

There are a number of mathematical models for the growth of biological tissue. The tissue is typically subdivided into a number of solid and fluid phases, and the dynamics are described by equations for the volume fractions, velocities and pressures of each phase. The governing equations are often analogous to those used in geophysical models (*e.g.* compaction in sedimentary basins [7]). They consist of equations expressing the conservation of mass of each phase, Darcy's Law (relating the velocities to the pressure gradients) and a force balance involving a constitutive law for the rheology of the medium.

Models for articular cartilage [13] and solid tumours [14] divide the tissue into a single solid phase and an interstitial fluid phase. However, in the problem with which we are concerned, cells within the different regions of the growth plate vary considerably in size and number, and to account for this, we present a triphasic model consisting of cartilage cells, solid matrix and interstitial fluid.

The columnar structure of cells in the growth plate is readily discernible (see Fig. 1.3 (B)), suggesting that bone elongation is due to the co-ordinated growth of individual columns, with cells at the same height in neighbouring columns having similar size and behaviour. An idealized view (Fig. 2.1) used by experimentalists implies that we

can account for bone growth by considering just one column of cells: accordingly, we present a one-dimensional model for growth plate dynamics.

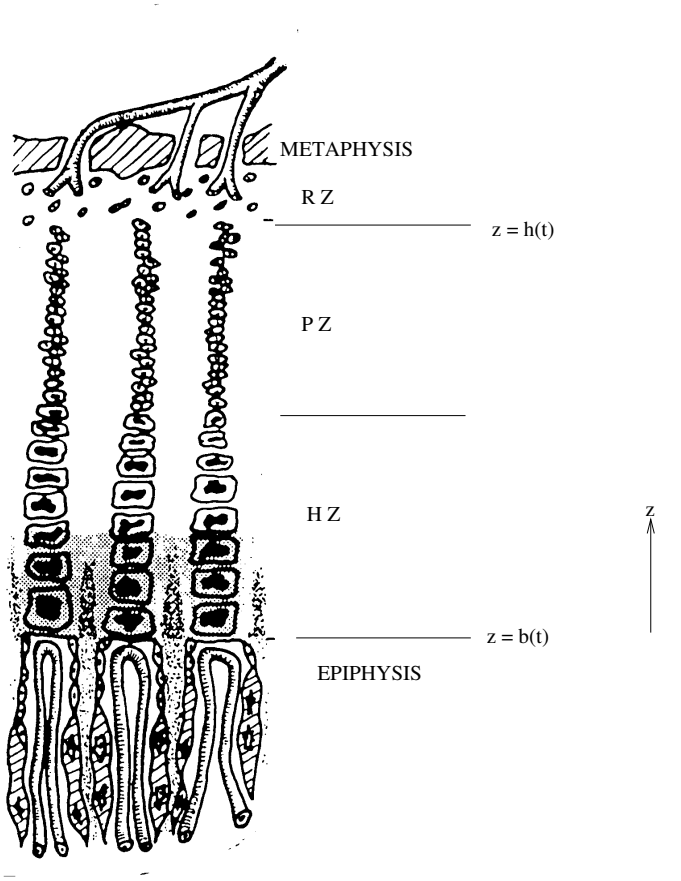


Figure 2.1: Schematic showing the zones of the growth plate and positions of the base ($z = b(t)$) and top ($z = h(t)$).

2.2 Derivation of the governing equations

Let z be our spatial variable, defined in the direction of longitudinal growth. The point $z = b(t)$ denotes the position of the chondro-osseous junction, and $z = h(t)$ denotes the top of the proliferative zone, *i.e.* the height at which chondrocytes begin mitosis. Let ϕ^c represent the volume fraction of cells, ϕ^m the volume fraction of solid matrix, and ϕ^f that of the interstitial fluid. Then for any given volume of the growth plate we have

$$\phi^c + \phi^m + \phi^f = 1. \tag{2.1}$$

Let ρ^c, ρ^m, ρ^f be the densities of each phase, which we assume to be constant. We denote by u^f the velocity of the fluid, and the velocity of the cells and the matrix by u^s. Since each cell synthesizes its own 'coat' of matrix, it seems reasonable to assume that this coat will move along with the cell, or at least that any relative motion between cell and solid matrix will be negligible compared with their motion relative to the surrounding fluid.

For each phase we have an equation expressing conservation of mass. Consider the general case of a phase with constant density ρ and volume fraction ϕ, moving with velocity u in an arbitrary volume V of the growth plate, with boundary ∂V. Then

$$\frac{d}{dt}\int_V \rho\phi dV = -\int_{\partial V} \boldsymbol{J}.d\boldsymbol{S} + \int_V L dV. \tag{2.2}$$

The expression on the left-hand side represents the rate of change of the amount of the phase in V. $\boldsymbol{J}$ is the fluid flux through ∂V, given in one dimension by

$$J = \rho\phi u. \tag{2.3}$$

L is the net production of the phase in V.

Applying the Divergence Theorem to (2.2), and noting that V is arbitrary, we have

$$\rho(\phi_t + (\phi u)_z) = L, \tag{2.4}$$

where subscripts denote partial derivatives.

Applying this argument to our three phases, we obtain the following three conservation equations for ϕ^f, ϕ^c and ϕ^m:

$$\rho^f(\phi^f_t + (\phi^f u^f)_z) = 0, \tag{2.5}$$

$$\rho^c(\phi^c_t + (\phi^c u^s)_z) = R^c\rho^c\phi^c, \tag{2.6}$$

$$\rho^m(\phi^m_t + (\phi^m u^s)_z) = R^m\rho^m\phi^c. \tag{2.7}$$

In deriving (2.5) we have assumed for simplicity that there are no sources or sinks of fluid within the growth plate. In equations (2.6) and (2.7) we have assumed that proliferation and hypertrophic growth of cells are proportional to the volume fraction of cells, and similarly that matrix production and turnover occurs at a rate

proportional to ϕ^c. The production rates R^c and R^m are likely to be functions of nutrient concentration, and to depend on hormonal and growth factor concentrations within the growth plate: in the simplest case, though, we consider R^c and R^m to be constant.

Although there are a number of nutrients present in the growth plate, we consider, for simplicity, a single generic growth factor with concentration g. Conservation of mass of g can be expressed as

$$\frac{d}{dt}\int_V \phi^f g dV = -\int_{\partial V} \boldsymbol{J}.d\boldsymbol{S} - \int_V R dV, \tag{2.8}$$

where R is the uptake of nutrient by the chondrocytes. The flux of g is taken to be due to Fickian diffusion and advection; so in one dimension,

$$J = -\phi^f D g_z + \phi^f g u^f \tag{2.9}$$

where D is the diffusivity of g in the interstitial fluid. We define the uptake function R by

$$R = Y\phi^c. \tag{2.10}$$

Again for the simplest model, we consider the coefficient Y to be a constant. Hence, applying the Divergence Theorem to (2.8), we have

$$(\phi^f g)_t + (\phi^f g u^f)_z = (\phi^f D g_z)_z - Y\phi^c. \tag{2.11}$$

We describe conservation of liquid momentum by Darcy's Law [1],

$$\phi^f(u^f - u^s) = -\frac{k}{\mu}\frac{\partial p}{\partial z}, \tag{2.12}$$

where p is the pressure of the interstitial fluid, k is the permeability and μ is the viscosity.

We define the total stress on the growth plate by

$$\boldsymbol{\sigma} = -p\boldsymbol{I} + \boldsymbol{\sigma^E}, \tag{2.13}$$

where $\boldsymbol{\sigma^E}$ is the effective stress tensor of the solid phases and $\boldsymbol{I}$ is the unit tensor. Cohen *et. al.* [3] successfully described the compressive properties of the growth plate

[1] For a derivation of Darcy's Law, see [6].

by modelling the solid phases as transversely isotropic [2] about the z-axis. Following Terzaghi's [16] treatment of solid-fluid mixtures, we relate the effective stress to the strain tensor by a 4×4 stiffness matrix

$$\begin{pmatrix} \sigma^{rr} \\ \sigma^{\theta\theta} \\ \sigma^{zz} \\ \sigma^{zr} \end{pmatrix} = \begin{pmatrix} C_{11} & C_{12} & C_{13} & 0 \\ C_{12} & C_{11} & C_{13} & 0 \\ C_{13} & C_{13} & C_{33} & 0 \\ 0 & 0 & 0 & C_{44} \end{pmatrix} \begin{pmatrix} \epsilon^{rr} \\ \epsilon^{\theta\theta} \\ \epsilon^{zz} \\ \epsilon^{zr} \end{pmatrix} \tag{2.14}$$

where r, θ are polar coordinates in the transverse plane.

The coefficients in the matrix can be written in terms of the in- and out-of-plane Young's moduli (E_1, E_3 resp.), Poisson's ratios (ν_{21}, ν_{31}) and the out-of-plane shear modulus G_{31} (see [12] for definitions of these quantities):

$$\begin{aligned} C_{11} &= \frac{E_1(1-\nu_{31}^2\frac{E_1}{E_3})}{(1+\nu_{21})\Delta} \\ C_{12} &= \frac{E_1(\nu_{21}+\nu_{31}^2\frac{E_1}{E_3})}{(1+\nu_{21})\Delta} \\ C_{13} &= \frac{E_1\nu_{31}}{\Delta} \\ C_{33} &= E_3(1+2\nu_{31}^2\frac{E_1}{E_3\Delta}) \\ C_{44} &= 2G_{31} \end{aligned} \tag{2.15}$$

where

$$\Delta = 1-\nu_{21}-2\nu_{31}^2\frac{E_1}{E_3}. \tag{2.16}$$

Experimentally, Cohen *et. al.* found that $\nu_{31} = 0$, so under conditions of uniaxial strain (where ϵ^{zz} is the only nonzero strain rate), (2.14) collapses to

$$\sigma^{zz} = E_3\epsilon^{zz}. \tag{2.17}$$

Now, assuming the limit of small strain, we have

$$\epsilon^{zz} = \frac{\partial w}{\partial z} \tag{2.18}$$

[2] *i.e.* if we consider any horizontal cross-section of the growth plate, each point will have the same elastic properties in the radial direction. However, due to the difference in cell numbers and size progressing down the growth plate, we must consider the growth plate to be anisotropic in the z-direction.

where w is the vertical displacement, and hence

$$u^s = \frac{\partial w}{\partial t}. \tag{2.19}$$

Therefore by (2.14)- (2.19), our one-dimensional constitutive relation is

$$\sigma = -p + E\frac{\partial w}{\partial z} \tag{2.20}$$

and a force balance tells us

$$\frac{\partial \sigma}{\partial z} = 0. \tag{2.21}$$

2.3 Boundary conditions at $z = h(t)$.

At a certain height, $z = h(t)$, in the growth plate cartilage, chondrocytes in the resting zone begin to divide. This switch to proliferative behaviour is assumed to occur when our generic growth factor g reaches some critical level, *i.e.* at

$$g = g_a, \tag{2.22}$$

for some non-negative constant g_a. This condition determines the position of the moving boundary $z = h(t)$.

We also specify the initial volume fraction of cells and solid matrix:

$$\phi^c = \phi_0^c, \qquad \phi^m = \phi_0^m. \tag{2.23}$$

Equation (2.1) then gives us the initial fluid volume fraction ϕ_0^f.

Similarly we specify the fluid pressure and the flux of g through $z = h$:

$$p = p_a = -\sigma, \tag{2.24}$$

$$\phi^f g u^f - \phi^f D g_z = -J_a, \tag{2.25}$$

where p_a and J_a are non-negative constants.

2.4 Boundary conditions at $z = b(t)$.

$z = b(t)$ is the position at which all chondrocytes die and are replaced by bone. We assume that this occurs when cells are starved of g, *i.e.* when

$$g = 0. \tag{2.26}$$

We wish to specify the velocities of the solid and fluid phases at the base of the growth plate. Physically, any unmineralized material at the bone front is broken down and replaced by bone-forming material, with only the mineralized solid matrix remaining. We assume that as the bone front advances, the fluid and solid phases are 'frozen' in its wake, so that

$$u^s = u^f = 0 \qquad \text{in } z < b(t). \tag{2.27}$$

A conservation principle applied to the fluid and the combined solid phases respectively across $z = b(t)$ tells us that

$$\dot{b}(t) \left[\phi^f\right]_-^+ = \left[\phi^f u^f\right]_-^+ \tag{2.28}$$

and

$$\dot{b}(t) \left[1 - \phi^f\right]_-^+ = \left[(1 - \phi^f)u^s\right]_-^+ . \tag{2.29}$$

Naturally, once the cells die, matrix production and hypertrophic growth cease, so the volume fractions of each phase remain unchanged, and hence continuous, across the front. Equations (2.28) and (2.29), together with (2.27), then imply that at $z = b^+$,

$$u^f = u^s = 0. \tag{2.30}$$

We also specify zero flux of g through $z = b$, so that

$$\phi^f g u^f - \phi^f D g_z = 0. \tag{2.31}$$

2.5 Nondimensionalisation

We nondimensionalize g by the concentration of g at the top of the growth plate, so from (2.22),

$$g = g_a g^*. \tag{2.32}$$

Similarly (2.24) and (2.20) give us a pressure scale

$$p - p_a = Ep^*. \tag{2.33}$$

We choose a length scale such that, in the steady state, the diffusion term balances the uptake term on the right-hand side of (2.11). Therefore

$$z = lz^*, \tag{2.34}$$

where l is obtained from the relation

$$\frac{Dg_a}{l^2} = Y. \tag{2.35}$$

Using the conservation equation (2.6), we choose a timescale defined by the inverse of the cellular production rate

$$t = t_0 t^*, \tag{2.36}$$

where

$$t_0 = \frac{1}{R^c}. \tag{2.37}$$

In the more realistic case of R^c being a variable, we take $t_0 = \frac{1}{R^c_{typ}}$, R^c_{typ} being a typical size of the cellular production rate.

We are now in a position to nondimensionalize the remaining quantities:

$$u^s = \frac{l}{t_0} u^{s*}, \qquad u^f = \frac{l}{t_0} u^{f*} \tag{2.38}$$

$$b(t) = lb^*(t^*), \qquad h(t) = lh^*(t^*) \tag{2.39}$$

$$R^m = \frac{1}{t_0} R^{m*}. \tag{2.40}$$

In terms of the nondimensionalized quantities, and dropping asterisks for convenience, the model takes the form

$$\phi^c + \phi^m + \phi^f = 1 \tag{2.41}$$

$$\phi^f_t + (\phi^f u^f)_z = 0 \tag{2.42}$$

$$\phi^c_t + (\phi^c u^s)_z = \phi^c \tag{2.43}$$

$$\phi^m_t + (\phi^m u^s)_z = \Gamma \phi^c \tag{2.44}$$

$$\mathrm{Pe}[(\phi^f g)_t + (\phi^f g u^f)_z] = (\phi^f g_z)_z - \phi^c \tag{2.45}$$

$$\phi^f (u^f - u^s) = -\lambda \frac{\partial p}{\partial z} \tag{2.46}$$

$$p = \frac{\partial w}{\partial z}, \tag{2.47}$$

for $z \in [b(t), h(t)]$, $t \in [0, \infty)$, where

$$u^s = \frac{\partial w}{\partial t}. \tag{2.48}$$

Nondimensionalising the boundary conditions yields,

at $z = h(t)$,

$$g = 1, \tag{2.49}$$

$$\phi^c = \phi_0^c, \qquad \phi^m = \phi_0^m, \tag{2.50}$$

$$p = 0, \tag{2.51}$$

$$\mathrm{Pe}(\phi^f g u^f) - \phi^f g_z = -\alpha, \tag{2.52}$$

and at $z = b(t)$

$$u^s = u^f = 0, \tag{2.53}$$

$$\mathrm{Pe}(\phi^f g u^f) - \phi^f g_z = 0, \tag{2.54}$$

$$g = 0. \tag{2.55}$$

We now have seven equations for the variables ϕ^f, ϕ^c, ϕ^m, u^s, u^f, g and p. Expression (2.50) gives us two boundary conditions for ϕ^c, ϕ^m, which together with (2.41) tells us ϕ^f at $z = h(t)$. (2.53) gives us two boundary conditions for u^s and u^f, (2.51) is the boundary condition for p, and (2.52), (2.54) are the two conditions required to solve equation (2.45) for g. The two 'extra' boundary conditions, (2.49) and (2.55), are the kinematic boundary conditions for the moving boundaries $z = h(t)$ and $z = b(t)$.

The dimensionless parameters arising in the model are

$$\Gamma = \frac{R^m}{R^c}, \tag{2.56}$$

$$\mathrm{Pe} = \frac{l^2}{t_0 D}, \tag{2.57}$$

$$\lambda = \frac{kEt_0}{\mu l^2}, \tag{2.58}$$

$$\alpha = \frac{J_a l}{D g_a}. \tag{2.59}$$

2.6 Sizes of the dimensionless parameters.

Cohen's [3] experiments on the distal ulnae of four-month-old calves suggest the following approximate values for the out-of-plane Young's modulus and permeability coefficient:

$$E \approx 0.5 \times 10^6 \text{ Pa} \tag{2.60}$$

$$\frac{k}{\mu} \approx 3.4 \times 10^{15} \text{ m}^4 \text{ N}^{-1} \text{ s}^{-1} \tag{2.61}$$

For the diffusivity of g, we use the diffusivity of glucose in the interstitial fluid:

$$D \approx 10^{-10} \text{ m}^2 \text{ s}^{-1}. \tag{2.62}$$

Experimentally, it is very difficult to measure quantities such as the uptake of nutrient (Y) and the cellular production rate R^c. It is much simpler to determine length- and timescales in the growth plate by direct measurement. We choose our length scale to be the typical distance from the top of the proliferative zone to the base of the growth plate in large mammals (including humans and cows), i.e.

$$l \approx 10^{-3} \text{ m}. \tag{2.63}$$

Similarly, we choose the timescale to be the average lifespan of a chondrocyte within the growth plate, i.e.

$$t_0 \approx 3 \times 10^5 \text{ s}. \tag{2.64}$$

Implicit in choosing these values is the assumption that they are consistent with the scales implied by (2.35), (2.37) were we able to quantify the other parameters involved in these expressions.

Substituting these values into (2.57) and (2.58), we have

$$\text{Pe} \approx \frac{(10^{-3})^2}{3 \times 10^5 . 10^{-10}} \approx 0.03 \tag{2.65}$$

and

$$\lambda \approx \frac{3.4 \times 10^{-15}.0.5 \times 10^{6}.3 \times 10^{5}}{(10^{-3})^2} \approx 500. \tag{2.66}$$

The nondimensionalisation was chosen to make the variables O(1). The fact that $\mathrm{Pe} \ll 1$ gives us as a leading-order approximation to (2.45)

$$(\phi^f g_z)_z \approx \phi^c, \tag{2.67}$$

with approximate boundary conditions

$$\phi^f g_z \approx 0 \qquad \text{at } z = b \tag{2.68}$$

and

$$\phi^f g_z \approx \alpha \qquad \text{at } z = h. \tag{2.69}$$

Integrating (2.67) with respect to z and using these boundary conditions, we find

$$\alpha \approx \int_b^h \phi^c dz. \tag{2.70}$$

The right-hand side of this expression contains only O(1) terms, so we deduce that α is also O(1).

The final dimensionless parameter, Γ, which represents the ratio of matrix to cell production, is also assumed to be O(1), since experiments on rats by Wilsman, Farnum et. al. [18], and Hunziker [11] show that the contribution of matrix synthesis to daily growth (relative to the contribution from cellular proliferation and hypertrophy) at four different physes varies from 32 to 49%.

In summary we have four dimensionless parameters in the model: Γ, α of O(1), $\lambda \approx 500$ and $\mathrm{Pe} \approx 0.03$.

Chapter 3

Model Analysis

3.1 The leading-order model

From the previous chapter, we know $\lambda \gg 1$, so (2.46) tells us $\frac{\partial p}{\partial z} \ll 1$. This, together with (2.51) implies $p \ll 1$ throughout the growth plate, so (2.47) implies $w \ll 1$, and hence from (2.48) we have, as a leading-order approximation,

$$u^s \approx 0. \tag{3.1}$$

This tells us that the motion of cells and solid matrix is negligible compared with the speed at which bone is deposited.

Using (3.1) in (2.43), (2.44) gives

$$\phi^c_t \approx \phi^c, \tag{3.2}$$

$$\phi^m_t \approx \Gamma\phi^c, \tag{3.3}$$

and given the boundary condition $\phi^c = \phi^c_0$ at $z = h(t)$, we can solve (3.2) to obtain

$$\phi^c = \phi^c_0 e^{t-h^{-1}(z)}. \tag{3.4}$$

Hence (3.3) becomes

$$\phi^m_t \approx \Gamma\phi^c_0 e^{t-h^{-1}(z)}, \tag{3.5}$$

which with the boundary condition $\phi^m = \phi^m_0$ at $z = h(t)$ gives

$$\phi^m = \Gamma\phi^c_0(e^{t-h^{-1}(z)} - 1) + \phi^m_0. \tag{3.6}$$

Equation (2.41) then gives us ϕ^f.

From the previous chapter we know

$$(\phi^f g_z)_z \approx \phi^c, \tag{3.7}$$

and so from (3.4), we have

$$(\phi^f g_z)_z = \phi_0^c e^{t-h^{-1}(z)} \tag{3.8}$$

with the two boundary conditions

$$\phi^f g_z = \alpha \qquad \text{at } z = h(t) \tag{3.9}$$

and

$$\phi^f g_z = 0 \qquad \text{at } z = b(t). \tag{3.10}$$

We have two further boundary conditions

$$g = 1 \qquad \text{at } z = h(t) \tag{3.11}$$

and

$$g = 0 \qquad \text{at } z = b(t), \tag{3.12}$$

which specify the positions of the moving boundaries.

3.2 Steady state solution

Over a period of days, bone growth can be thought of as steady, in that the thickness of the growth plate remains approximately constant, and new bone is deposited at a constant speed. Hence we shall look for a travelling wave-type solution to our leading-order problem, where the top of the growth plate moves with a constant speed v. Accordingly we define

$$h = vt \tag{3.13}$$

and make the change of variable

$$Z = vt - z. \tag{3.14}$$

Under this transformation the equations become

$$\phi^c = \phi_0^c e^{Z/v}, \tag{3.15}$$

$$\phi^m = \phi_0^m + \Gamma\phi_0^c(e^{Z/v} - 1), \tag{3.16}$$

and

$$(\phi^f g_Z)_Z = \phi_0^c e^{Z/v}, \tag{3.17}$$

with boundary conditions

$$\phi^f g_Z = -\alpha, \qquad g = 1 \qquad \text{at } Z = 0 \tag{3.18}$$

and

$$\phi^f g_Z = 0, \qquad g = 0 \qquad \text{at } Z = B(t). \tag{3.19}$$

$B(t) = vt - b$ is the thickness of the growth plate.

Integrating (3.17) from 0 to Z yields

$$\begin{aligned} \phi^f g_Z + \alpha &= \int_0^Z \phi_0^c e^{\zeta/v} d\zeta \\ &= v\phi_0^c(e^{Z/V} - 1), \end{aligned} \tag{3.20}$$

so when $Z = B(t)$ we have

$$\alpha = v\phi_0^c(e^{B/v} - 1) \tag{3.21}$$

$$\Rightarrow B = v\log(\frac{\alpha}{v\phi_0^c} + 1). \tag{3.22}$$

This gives us a relation between the growth plate thickness, B, and the rate of growth v.

Now, assuming that the volume fraction of fluid remains nonzero throughout the growth plate, (3.20) tells us that

$$\frac{dg}{dZ} = \frac{v\phi_0^c(e^{Z/v} - 1) - \alpha}{1 - (1+\Gamma)\phi_0^c e^{Z/v} - \phi_0^m + \Gamma\phi_0^c}, \tag{3.23}$$

so using (3.21), we have

$$\frac{dg}{dZ} = \frac{-v\phi_0^c(e^{B/v} - e^{Z/v})}{1 + \Gamma\phi_0^c - \phi_0^m - (1+\Gamma)\phi_0^c e^{Z/v}}. \tag{3.24}$$

Integrating with respect to Z gives us

$$g - 1 = -\frac{v}{1+\Gamma}\int_0^Z \frac{a_1 - e^{\zeta/v}}{a_2 - e^{\zeta/v}} d\zeta, \tag{3.25}$$

where

$$a_1 = e^{B/v} \tag{3.26}$$

$$= 1 + \frac{\alpha}{v\phi_0^c} \qquad \text{by (3.21)}, \tag{3.27}$$

and

$$a_2 = \frac{1 + \Gamma\phi_0^c - \phi_0^m}{(1+\Gamma)\phi_0^c} \tag{3.28}$$

$$= 1 + \frac{\phi_0^f}{(1+\Gamma)\phi_0^c}. \tag{3.29}$$

The requirement that v and Γ are non-negative, and that $g \in [0, 1]$, tells us that the denominator of the integrand in (3.25) must also be non-negative, *i.e.*

$$a_2 \geq e^{\zeta/v}, \qquad \forall \zeta \in [0, B] \tag{3.30}$$

and hence

$$a_2 \geq a_1. \tag{3.31}$$

From the definitions of a_1 and a_2, we have the solvability condition

$$1 + \frac{\phi_0^f}{(1+\Gamma)\phi_0^c} \geq 1 + \frac{\alpha}{v\phi_0^c}, \tag{3.32}$$

$$\Rightarrow v \geq \frac{\alpha(1+\Gamma)}{\phi_0^f}. \tag{3.33}$$

This tells us that there is a non-zero minimum wavespeed at which steady growth can occur, *i.e.*

$$v_0 = \frac{\alpha(1+\Gamma)}{\phi_0^f}. \tag{3.34}$$

When $v = v_0$, and hence $a_1 = a_2$, (3.25) trivially integrates to

$$g - 1 = -\frac{vZ}{1+\Gamma}. \tag{3.35}$$

Using boundary condition (3.19) tells us

$$1 = \frac{v_0 B}{1+\Gamma}. \tag{3.36}$$

Hence we have a minimum growth plate thickness for which steady growth can occur, which, using (3.34), is given by

$$B_0 = \frac{\phi_0^f}{\alpha}. \tag{3.37}$$

Now, returning to the case $a_2 > a_1$, we can rewrite the integrand in (3.25) as $1 - \frac{a_2 - a_1}{a_2 - e^{\zeta/v}}$, which yields

$$g - 1 = -\frac{vZ}{1+\Gamma} + \frac{v(a_2 - a_1)}{1+\Gamma} \int_0^Z \frac{d\zeta}{a_2 - e^{\zeta/v}}. \tag{3.38}$$

Changing variables to $y = e^{\zeta/v}$ gives

$$\begin{aligned} g - 1 &= -\frac{vZ}{1+\Gamma} + \frac{v^2(a_2 - a_1)}{1+\Gamma} \int_1^{e^{Z/v}} \frac{dy}{y(a_2 - y)} && (3.39)\\ &= vB - \frac{v^2(a_2 - a_1)}{a_2} \int_1^{e^{Z/v}} (\frac{1}{y} + \frac{1}{a_2 - y}) dy && (3.40)\\ &= -\frac{vZ}{1+\Gamma} + \frac{v^2(a_2 - a_1)}{(1+\Gamma)a_2} \left[\frac{Z}{v} - \log(a_2 - e^{Z/v}) + \log(a_2 - 1) \right] && (3.41)\\ &= -\frac{a_1 vZ}{(1+\Gamma)a_2} + \frac{v^2(a_2 - a_1)}{(1+\Gamma)a_2} \log\left(\frac{a_2 - 1}{a_2 - e^{Z/v}} \right). && (3.42) \end{aligned}$$

After some manipulation, this can be written in terms of the original variables as

$$g = 1 - Z\left(\frac{\alpha + v\phi_0^c}{(1+\Gamma)\phi_0^c + \phi_0^f} \right) + \frac{v(v\phi_0^f - (1+\Gamma)\alpha)}{(1+\Gamma)((1+\Gamma)\phi_0^c + \phi_0^f)} \log\left(\frac{\phi_0^f}{\phi_0^f - (1+\Gamma)\phi_0^c(e^{Z/v} - 1)} \right). \tag{3.43}$$

Substituting in the boundary condition at $Z = B$ gives us a second relation between v and B:

$$(1+\Gamma)\phi_0^c + \phi_0^f = B(\alpha + v\phi_0^c) + \frac{v}{1+\Gamma}(v\phi_0^f - (1+\Gamma)\alpha) \log\left(1 - \frac{(1+\Gamma)\alpha}{v\phi_0^f} \right). \tag{3.44}$$

We can simplify this relation by substituting for α, Γ, ϕ_0^c and ϕ_0^f in terms of v_0 and B_0. Note first of all that (3.21) tells us

$$\frac{\alpha}{\phi_0^c} = v_0(e^{B_0/v_0} - 1). \tag{3.45}$$

If we now divide (3.44) through by α, we get

$$\frac{B_0 v_0}{v_0(e^{B_0/v_0}-1)} = B\left(1+\frac{v}{v_0(e^{B_0/v_0}-1)}\right)+\frac{v}{v_0 B_0}(vB_0 - v_0 B_0)\log\left(1-\frac{v_0}{v}\right) \quad (3.46)$$

$$\Rightarrow B_0 v_0 e^{B_0/v_0} = B(v_0(e^{B_0/v_0}-1)+v)+v(e^{B_0/v_0}-1)(v-v_0)\log\left(1-\frac{v_0}{v}\right), \quad (3.47)$$

where B is given by

$$B = v\log\left(\frac{v_0(e^{B_0/v_0}-1)}{v}+1\right). \quad (3.48)$$

Now let

$$\eta = \frac{1}{e^{B_0/v_0}-1} = \frac{(1+\Gamma)\phi_0^c}{\phi_0^f} \quad (3.49)$$

and

$$\hat{v} = \frac{\eta v}{v_0} = \frac{v\phi_0^c}{\alpha}. \quad (3.50)$$

Then dividing each side of (3.47) by v^2 yields

$$\frac{\eta^2}{\hat{v}^2}\left(\frac{1}{\eta}+1\right)\log\left(\frac{1}{\eta}+1\right) = \left(\frac{1}{\hat{v}}+1\right)\log\left(\frac{1}{\hat{v}}+1\right)+\frac{1}{\eta}\left(1-\frac{\eta}{\hat{v}}\right)\log\left(1-\frac{\eta}{\hat{v}}\right), \quad (3.51)$$

i.e.

$$\eta(1+\eta)\log\left(1+\frac{1}{\eta}\right) = \hat{v}\left[(1+\hat{v})\log\left(1+\frac{1}{\hat{v}}\right)+\frac{1}{\eta}(\hat{v}-\eta)\log\left(1-\frac{\eta}{\hat{v}}\right)\right]. \quad (3.52)$$

Using MAPLE's `implicitplot` command, we plot $v = \frac{\alpha}{\phi_0^c}\hat{v}(\eta)$ against η (Fig. 3.1). From the plot it can be seen that increasing η, and hence increasing Γ, results in an increased rate of growth, while increasing α will result in a reduced growth rate. The velocities also seem to approach infinity as η approaches some critical value η_{crit}. We can determine this value by expanding the logarithms in (3.52) in powers of $\frac{1}{\hat{v}}$ as $v \to \infty$. This results in

$$\eta_{crit}\log\left(1+\frac{1}{\eta_{crit}}\right) = \frac{1}{2}, \quad (3.53)$$

and by a simple iteration we obtain the value

$$\eta_{crit} \approx 0.398. \quad (3.54)$$

Hence it appears that while there is a minimum velocity at which steady growth can occur, there is no upper limit on the velocity. We also have an upper limit on Γ (the ratio of matrix to cell production) after which steady growth is impossible:

$$\Gamma < \Gamma_{crit} = \frac{0.398\phi_0^f}{\phi_0^c}, \quad (3.55)$$

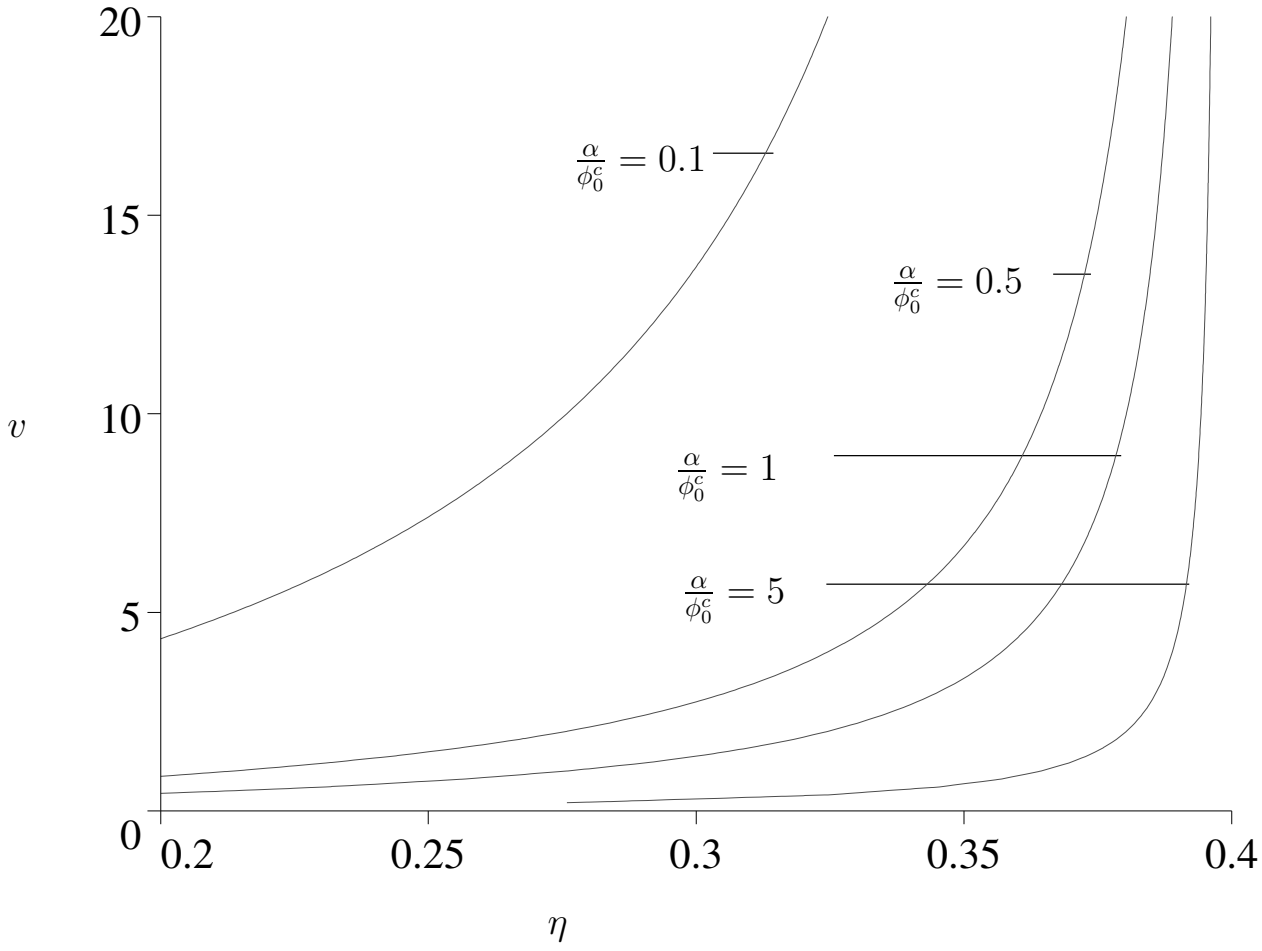


Figure 3.1: Graph of growth rate versus the parameter η for various values of α.

and since Γ must also be non-negative, we have

$$\phi_0^c < 0.398\,\phi_0^f. \tag{3.56}$$

We are now in a position to seek values of the parameters ϕ_0^c, ϕ_0^f, Γ, α, v and B which satisfy the numerous steady state criteria. If we choose ϕ_0^c, ϕ_0^f and Γ, we can use the plots in Fig. 3.1 to find suitable values of v and α, and hence B (from equation (3.22)). We now present plots of the variations in the volume fractions of each phase (Fig. 3.2), and in the concentration of g (Fig. 3.3) from the top to the base of the growth plate. The parameter values we have chosen are:

$$\phi_0^c = 0.2$$

$$\phi_0^f = 0.7$$

$$\Gamma = 0.3$$

$$\alpha = 0.57$$

$$B = 1.77 \Rightarrow B_{dim} = 1.77 \times 10^{-3} \text{ m}$$

$$v = 2 \Rightarrow v_{dim} = 0.67 \times 10^{-8} \text{ m s}^{-1}.$$

Note that all these values are consistent with the assumption that α and Γ are of a similar size to the model variables, and hence should be included in the leading-order model.

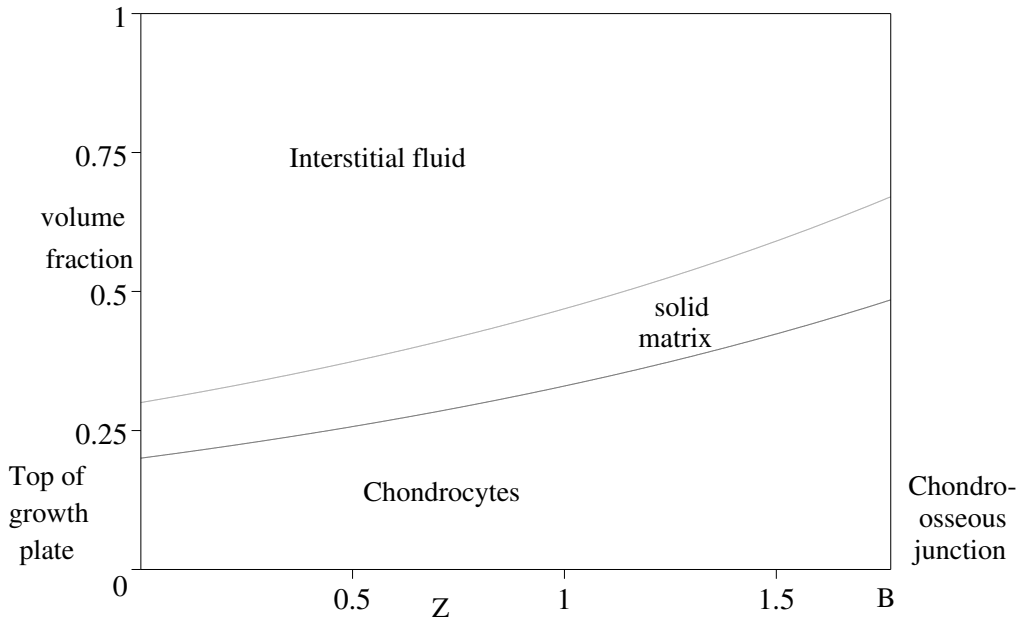


Figure 3.2: Graph showing the volume fractions of each phase in the growth plate for typical values of steady-state parameters

3.3 Comparison with data

There are two data sets for growth rates and total growth plate thickness. Wilsman *et. al.* [18] considered four different physes of twelve male 28-day-old Long-Evans rats, while Hunziker and Schenk [11] considered the same physis of 18 female Wistar rats from three different age groups. Their data is summarized in the tables below,

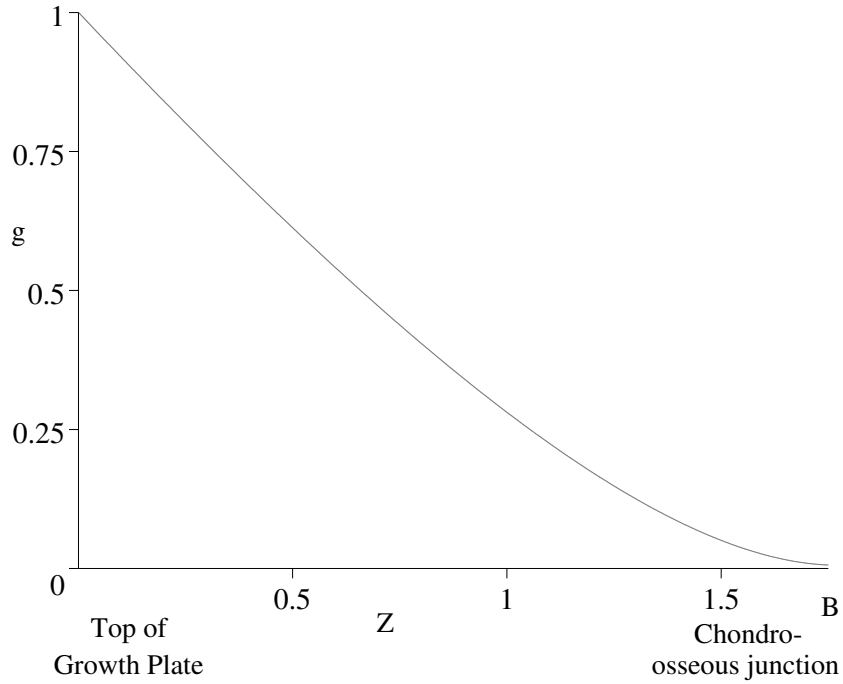


Figure 3.3: Graph showing the concentration of growth factor g in the growth plate interstitial fluid.

and α is calculated from (3.21), taking $\phi_0^c = 0.24$ as the initial cell volume fraction in each growth plate.

Physis	v_{dim} (μm/day)	B_{dim} (μm)	v	B	α
Prox. rad	396	619	1.375	0.619	0.188
Dist. rad	269	515	0.934	0.515	0.165
Prox. tib	138	326	0.479	0.326	0.112
Dist. tib	47	181	0.163	0.181	0.080

age (days)	v_{dim} (μm/day)	B_{dim} (μm)	v	B	α
21	276	653	0.958	0.653	0.225
35	330	583	1.146	0.583	0.182
80	85	216	0.295	0.216	0.076

Again using (3.21), we plot curves of B versus v (Fig. 3.4) for three values of α: the maximum and minimum values of α calculated from the data, and the mean of

the α's. The data points are plotted as empty boxes. Having only seven data points to analyse, it is difficult to come to any meaningful conclusions, other than that increasing α while keeping v fixed results in increased thickness of the growth plate, and similarly fixing B confirms that v decreases with increasing α. The calculated values of α are, encouragingly, of a comparable size to v and B.

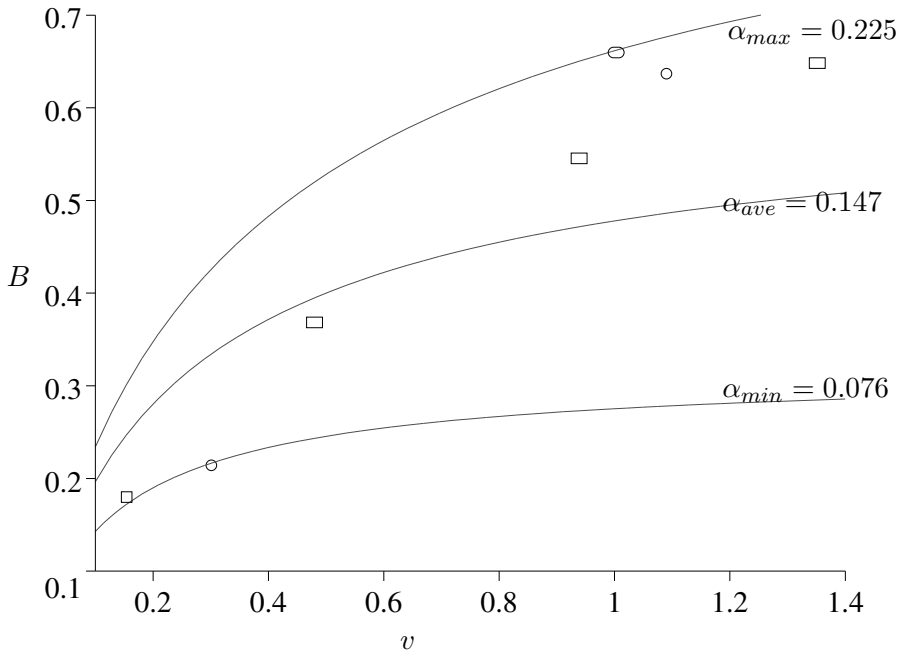


Figure 3.4: Graph showing the relationship between v and B for three values of α.

Chapter 4

Discussion and Conclusion

4.1 Review of dissertation

In this dissertation we have presented a simplified, one-dimensional model for longitudinal bone growth, where the growth plate cartilage is considered to consist of a cellular phase, solid matrix, and an interstitial fluid phase. We have postulated that a generic growth factor g is responsible for the onset of cellular proliferation, hypertrophy and cell death at the chondro-osseous junction. In nondimensionalising, we have found that the model depends on two key parameters:

$$\Gamma = \frac{R^m}{R^c}$$

and

$$\alpha = \frac{J_a l}{D g_a},$$

both of which are assumed to be O(1).

Analysis of the steady state model produced two equations for the steady growth rate v and the growth plate thickness B in terms of Γ and α. Steady growth was found to be possible for realistic values of the model parameters, with certain restrictions (*i.e.* there exist minimum values of v and B, and a maximum value of Γ for which steady growth can occur). The model is consistent with the observation that a range of growth rates occur at different growth plates in the body, and indicates that, in theory, an arbitrarily high growth speed can be attained.

The growth rate was shown to be an increasing function of Γ (for $\Gamma < \Gamma_{crit}$). This seems plausible, as one would expect that an increase in the rate of matrix synthesis per cell would result in faster displacement of the top of the proliferative zone. Similarly, v was shown to decrease as α is increased. Note that α is inversely proportional to g_a, which suggests that an augmented nutrient supply to the growth plate will result in faster growth.

4.2 Model limitations and directions for future research

While the model captures the qualitative behaviour of steady bone growth, we have made many oversimplifications. A more sophisticated model would distinguish between proliferative and hypertrophic contributions to growth. One way of modelling this is to decompose the volume fraction of cells into the product of a cell number density and cell volume, *i.e.*

$$\phi^c = n^c V^c. \tag{4.1}$$

If the transition from proliferative to hypertrophic behaviour occurs at a critical level of the growth factor, g_{crit}, we can write down conservation of mass of cells in the two regions $g > g_{crit}$ and $g < g_{crit}$ analogous to equation (2.6). For $g > g_{crit}$ we have

$$n^c_t + (n^c u^s)_z = r n^c. \tag{4.2}$$

We have assumed that the cell volume in the proliferative zone remains constant, and that the only source of cell mass is the production of cells by mitosis. We can define r by

$$r = \frac{1}{t^c}, \tag{4.3}$$

where t^c is the cell cycle time (the time between two successive divisions of the same cell).

Similarly in $g < g_{crit}$ we have

$$V^c_t + (V^c u^s)_z = G(g), \tag{4.4}$$

where we assume that the number of cells in the hypertrophic zone is constant, and that the rate of volume increase is a function of g.

Another unrealistic assumption of our model is that the production rates of cells and matrix, and the uptake of g by cells, is not dependent on g. An interesting development would be to make Γ and α in the steady state model g-dependent. When bone growth is monitored over a long period of time, pubertal 'growth spurts' are observed at irregular intervals. It is possible that these fluctuations in growth are the result of a g-dependent oscillation about a steady state.

In order to formulate a realistic model for bone growth, we need to better our understanding of the intrinsic cellular processes that occur in the growth plate. The rate and amount of matrix production per cell is poorly documented, and debate still occurs over the fate of chondrocytes at the chondro-osseous junction. From a mathematical perspective, it would be useful to be able to quantify the concentration of nutrients in each region of the growth plate, as well as to define more clearly the role of mechanical stresses and strains in controlling growth.

Bibliography

[1] J. Aronson. Temporal and spatial increases in blood flow during distraction osteogenesis. *Clin. Orthop.*, 301:124–131, 1994.

[2] G.J. Breur, B.A. VanEnkevort, C.E. Farnum, and N.J. Wilsman. Linear relationship between the volume of hypertrophic chondrocytes and the rate of longitudinal bone growth in growth plates. *J. Orthop. Res.*, 9:348–359, 1991.

[3] B. Cohen, W.M. Lai, and V.C. Mow. A transversely isotropic biphasic model for unconfined compression of growth plate and chondroepiphysis. *J. Biomech. Eng.*, 120:491–496, 1998.

[4] C.E. Farnum and N.J. Wilsman. Effects of distraction and compression on growth plate function. In J.A. Buckwalter, M.G. Ehrlich, L.J. Sandell, and S.B. Trippel, editors, *Skeletal Growth and Development*, pages 517–531. AAOS, Rosemont, Illinois, 1997.

[5] C.E. Farnum and N.J. Wilsman. Growth plate cellular function. In J.A. Buckwalter, M.G. Ehrlich, L.J. Sandell, and S.B. Trippel, editors, *Skeletal Growth and Development*, pages 203–223. AAOS, Rosemont, Illinois, 1997.

[6] A.C. Fowler. *Mathematical Models in the Applied Sciences*. Cambridge University Press, Cambridge, 1998.

[7] A.C. Fowler and X. Yang. Fast and slow compaction in sedimentary basins. *SIAM J. Appl. Math.*, 59:365–385, 1998.

[8] R.N. Hensinger. An overview and clinical perspective of disturbances of skeletal morphogenesis and growth. In J.A. Buckwalter, M.G. Ehrlich, L.J. Sandell, and S.B. Trippel, editors, *Skeletal Growth and Development*, pages 379–395. AAOS, Rosemont, Illinois, 1997.

[9] E.B. Hunziker. Mechanism of longitudinal bone growth and its regulation by growth plate chondrocytes. *Microscopy Res. Tech.*, 28:505–519, 1994.

[10] E.B. Hunziker. Growth plate formation, structure and function. In J.A. Buckwalter, M.G. Ehrlich, L.J. Sandell, and S.B. Trippel, editors, *Skeletal Growth and Development*, pages 187–202. AAOS, Rosemont, Illinois, 1997.

[11] E.B. Hunziker and R.K. Schenk. Physiological mechanisms adopted by chondrocytes in regulating longitudinal bone growth in rats. *J. Physiol. (Lond.)*, 414:55–71, 1989.

[12] L.D. Landau and E.M. Lifshitz. *Theory of Elasticity*. Pergamon Press, Oxford, 1986.

[13] V.C. Mow, S.C. Kuei, W.M. Lai, and C.G. Armstrong. Biphasic creep and stress relaxation of articular cartilage in compression: theory and experiments. *J. Biomech. Eng.*, 102:73–84, 1980.

[14] P.A. Netti, L.T. Baxter, and Y. Boucher. Macro- and microscopic fluid transport in living tissues: application to solid tumors. *AIChE Journal*, 43:818–834, 1997.

[15] C. Ohlsson, J. Isgaard, J. Tornell, A. Nilsson, O.G.P. Isaksson, and A. Lindahl. Endocrine regulation of longitudinal bone growth. *Acta Paediatr. Suppl.*, 391:33–40, 1993.

[16] K. Terzaghi. *Theoretical Soil Mechanics*. John Wiley and Sons, New York, 1943.

[17] J. Trueta. *Studies of the Development and Decay of the Human Frame*. Heinemann Medical, London, 1968.

[18] N.J. Wilsman, C.E. Farnum, E.M. Leiferman, M. Fry, and C. Barreto. Differential growth by growth plates as a function of multiple parameters of chondrocytic kinetics. *J. Orthop. Res.*, 14:926–936, 1996.